EPR study of lipid phase in renal cortical membrane organelles from intact and cadmium-intoxicated rats

Zuvić-Butorac, Marta; Herak-Kramberger, M Carol; Krilov, Dubravka; Sabolić, Ivan; Herak, Janko

Source / Izvornik: **Biochimica et Biophysica Acta (BBA) - Biomembranes, 2005, 1718, 44 - 52**

Journal article, Published version
Rad u časopisu, Objavljena verzija rada (izdavačev PDF)

https://doi.org/10.1016/j.bbamem.2005.09.022

Permanent link / Trajna poveznica: https://urn.nsk.hr/urn:nbn:hr:193:688943

Available online at www.sciencedirect.com
SCIENCE DIRECT
Biochimica et Biophysica Acta 1718 (2005) 44 – 52
BIOCHIMICA ET BIOPHYSICA ACTA
BBA
http://www.elsevier.com/locate/bba

EPR study of lipid phase in renal cortical membrane organelles from intact and cadmium-intoxicated rats

Marta Žuvić-Butorac [a], Carol M. Herak-Kramberger [b], Dubravka Krilov [c], Ivan Sabolić [b], Janko N. Herak [d,*]

[a] *School of Medicine, University of Rijeka, Rijeka, Croatia*
[b] *Unit of Molecular Toxicology, Institute for Medical Research and Occupational Health, Zagreb, Croatia*
[c] *Department of Physics, Medical School, University of Zagreb, Zagreb, Croatia*
[d] *Division of Biophysics, Faculty of Pharmacy and Biochemistry, University of Zagreb, A. Kovačića 1, 10001 Zagreb, Croatia*

Received 15 July 2005; received in revised form 23 September 2005; accepted 27 September 2005
Available online 26 October 2005

Abstract

Numerous studies have demonstrated various structure/function correlations at the level of transport proteins in the kidney cell membranes and various intracellular organelles. However, characterization of the lipid phase of these membranes is rare. Here, we report the differences in lipid organization and dynamics of the brush-border membranes (BBM), basolateral membranes (BLM) and endocytotic vesicles (EV), isolated from the kidney cortex of intact rats, studied with the EPR spectroscopy of the spin-labeled membrane lipids. The EPR spectra were analyzed by comparing experimentally observed line shapes with the line shapes calculated according to the theoretical model developed for liquid crystals. In the fitting procedure, three different lipid domains were assumed, which revealed clear differences in the lipid ordering and rotational correlation times, as well as in the lipid partition of these domains in each of the three types of membranes. A similar approach, used to compare the spectroscopic characteristics of BBM from control and cadmium-intoxicated rats, showed significantly changed ordering and increased molecular mobility in the lipid phase of BBM from Cd-treated animals. As tested by an established fluorescence assay, the Cd-induced changes in the lipid mobility co localized with ~5-fold higher conductance of BBM for potassium, with unchanged conductance for protons.

Keywords: Basolateral membrane; Brush border membrane; Endocytic vesicle; EPR spectroscopy; Heavy metal nephrotoxicity; Ion conductance; Membrane fluidity

1. Introduction

Cadmium is an occupational and environmental toxic metal with potent nephrotoxic effects in humans and experimental animals. Nephrotoxicity induced by chronic exposition to cadmium is manifested by various structural and functional damages, largely in proximal tubules, that result in an acquired Fancony syndrome with a variety of urinary symptoms of the poor nephron functions, that include proteinuria, glucosuria, aminoaciduria, hyperosmolar polyuria, impaired secretion of organic anions, and increased fractional excretion of monovalent and divalent cations and anions [1–6]. Studies have shown that Cd-induced tubular disfunctions largely result from the loss of brush-border (BBM) and basolateral (BLM) membranes and their transporters and/or from direct or indirect inhibition of the activity of these transporters [2–14]. In our recent studies, we provided evidence that Cd can directly damage the integrity of plasma membranes and intracellular organelles, and decrease endocytosis and intracellular vesicle recycling of BBM transporters by damaging the activity of the V-ATPase and arrangement of cytoskeleton, thus leading to the overall loss of BBM structural and functional integrity [6,14–16].

Although the detailed mechanisms of Cd toxicity in mammalian kidneys is a subject of continuous investigation, it is notorious that most of the studies in this field so far have been conducted at the level of membrane transporters and various intracellular proteins, whereas lipid phase in the renal cell membranes and intracellular organelles has been seldom

* Corresponding author. Fax: +385 1 4856 201.
E-mail address: jaherak@pharma.hr (J.N. Herak).

0005-2736/$ - see front matter © 2005 Elsevier B.V. All rights reserved.
doi:10.1016/j.bbamem.2005.09.022

addressed [17]. Some biochemical studies of lipids in membranes of renal cortical brush border membranes (BBM), basolateral membranes (BLM), lysosomes, and endocytic vesicles (EV; endosomes), isolated from intact rats, were performed nearly 30 years ago [18]. That study exhibited clear differences in the relative content of various (phospho)lipids in the limiting membrane of these organelles. As shown in recent studies, in the mammalian kidney Cd induces oxidative stress and increases production of reactive oxidative species (ROS) that enhance peroxidation of lipids, however, in unspecified membranes and/or organelles [19–22]. These findings indicate that the lipid phase may play an important, but poorly defined role in intracellular onset and development of Cd (nephro)toxicity.

In order to provide information on structure and dynamics of the membrane lipid phase in renal membranes, which may be organelle-specific and compromised by Cd treatment, in this study, we first characterized the spin labeled lipid phase by the electron paramagnetic resonance (EPR) spectroscopy in various organelles from the kidney cortex of control rats. Thereafter, using optimal parameters, the EPR spectroscopic data for the renal cortical BBM from control and Cd-treated rats were compared and correlated with the membrane permeability for potassium and protons, determined by the acridine orange fluorescence quench method.

2. Materials and methods

2.1. Animals and treatment

Three-month-old male Wistar rats from the breeding colony at the Institute in Zagreb were used. Animals were bred and maintained according to the *Guide for Care and Use of Laboratory Animals* (Washington DC, Academic Press, 1996). Before and during experiments, animals had free access to standard laboratory food and tap water. The studies were approved by the Institutional Ethic Committee.

In accordance with our previous studies [6,13,15], Cd-nephrotoxicity was induced by injecting animals with a solution of $CdCl_2$ (2 mg Cd/kg b.w., s.c., daily for 2 weeks). Control animals received an equivalent amount (1 ml/kg b.w.) of vehicle (0.9% NaCl).

2.2. Isolation of membrane organelles from the kidney cortex

The rats were sacrificed by decapitation. The cortex of the removed kidneys was dissected manually. BBM, BLM, and endocytic vesicles were isolated from the cortical tissue homogenates by the established methods [23–25], using chilled buffers and the refrigerated high-speed centrifuge (Sorvall RC5C, rotor SS34). The transport and enzymatic characteristics of these membrane preparations were described previously [25,26]. As also proven previously [6], the isolated renal cortical BBM from control and Cd-treated rats are similarly enriched in the BBM marker leucine arylamidase (~14-fold) and the BLM marker Na/K-ATPase (~0.7-fold), indicating similar quality of the purified membranes. Isolated membranes were washed twice with, and finally prepared in KCl-buffer (150 mM KCl, 5 mM HEPES/Tris, pH 7.0) to the protein concentration of 13 mg/ml, and stored in liquid nitrogen until further use. Protein was measured by the Bradford assay [27], using bovine serum albumin as a standard.

2.3. Spin labeling

Frozen vesicles were thawed at 37 °C, diluted in a large volume of PBS (in mM: 140 NaCl, 4 KCl, 2 KH_2PO_4, pH 7.4), pelleted at 32,000×*g* for 30 min, dispersed in a small volume of PBS, and then incubated for 5 min with lipophilic spin probe, methyl ester of 5-doxyl palmitate MeFASL(10,3), Scheme 1.

The probe (synthesized by Prof. S. Pečar, Faculty of Pharmacy, University of Ljubljana), was uniformly distributed over the walls of the glass tube. The appropriate number of spin probe molecules was calculated to give final ratio of $N_{\text{spin probe}}/N_{\text{membrane lipid}}$=1:100. The labeled sample was washed three times with the probe-free PBS. The pellet was finally diluted in 50 μL PBS, transferred into a glass capillary (1 mm inner diameter) and the EPR spectra were immediately recorded on a Bruker ElexSys500 spectrometer (P=10 mW, v=9.3 GHz), at temperatures 22–42 °C, in steps of 5 °C.

2.4. ESR line shape evaluation

The EPR spectrum of lipid spin probe incorporated in the lipid bilayer can be calculated using the spin Hamiltonian, in which the organization and dynamics of neighboring molecules are considered to partially average the components of the interaction tensors. The formalism for the calculation of the spectrum was performed according to the model developed previously [28,29]. This model provides a set of fitting parameters that define the EPR line shape and at the same time give information on the structure and dynamics of the probed environment. Using the appropriate set of parameters, one can produce an EPR spectrum $\boldsymbol{s}(B)$ (B is magnetic field):

$$\boldsymbol{s}(B) = \boldsymbol{s}(S_1, S_3, \tau_{20}, \tau_{22}, B) \quad (1)$$

The order parameters S_3 and S_1 describe the average amplitude of motion (or time averaged position) of the long molecular axis of the nitrogen 2pπ orbital, relative to the bilayer normal and perpendicular to the bilayer normal, respectively, while rotational correlation times τ_{22} and τ_{20} refer to the rotation around and perpendicular to the long molecular axis of the spin label, respectively.

In applying the model to the analysis of the complex membrane spectra, we found that a reasonably good fit could be obtained employing three typical spectral components $\boldsymbol{s}_i(B)$, calculated by using Eq. (1), weighted and summed in the composite spectrum $\boldsymbol{S}(B)$:

$$\boldsymbol{S}(B) = \sum w_i \boldsymbol{s}_i(B) \quad (2)$$

$$\sum w_i = 1. \quad (3)$$

The weighting factors of the spectral components in the composite, calculated spectrum (that is to fit the experimental data), could be computed by the linear least squares approach in which the optimal values of w_i are evaluated through the maximum likehood of the least squares merit function. The goodness of the fit was deduced from the χ^2 value.

2.5. Fluorometric assay of ion conductances in BBM vesicles

The indirect fluorometric assay for studying K^+ and H^+ conductances in BBM vesicles (BBMV) was described in details previously [16,26]. The frozen BBM were thawed at 37 °C, left to equilibrate for 30 min in an ice bath, and vesiculated with 10 passages through the 25 G needle attached to a 1-ml syringe.

Generation and dissipation of transmembrane proton gradients in BBMV were monitored by fluorescence changes of acridine orange (AO), a ΔpH-sensitive dye that accumulates in acidic compartments. An aliquot of BBMV (20 μl, 260 μg protein) was added into 2.02 ml of TMACl-buffer (150 mM tetramethylammonium chloride, 5 mM HEPES/Tris, pH 7.0) that contained 6 μM AO, and either 2.5 μM valinomycin (K^+ ionophore) or 2.5 μM carbonyl

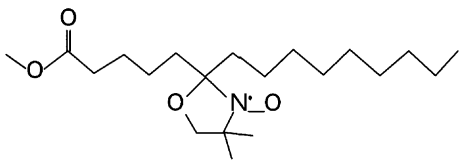

Scheme 1.

cyanide chloromethoxyphenylhydrazone (CCCP, H^+ ionophore) or both ionophores. This assay mixture was continuously stirred and heated at 37 °C, and the resulting fluorescence change was continuously recorded in a Shimatzu RF 510 spectrofluorometer ($\lambda_{ex}/\lambda_{em}$=493/525 nm). In these experimental conditions, e.g., having a steep transmembrane in-to-out K^+ gradient (approximately 102-fold difference) and high ionophore-mediated K^+ and H^+ conductances, the inside-negative K^+-diffusion potential was the driving force for intravesicular H^+ uptake by the ΔpH-dependent quenching of AO fluorescence. In the presence of valinomycin (unlimited K^+ conductance), the rate of fluorescence quenching (ΔQ/min) indicated the maximal intrinsic H^+ conductance of the membrane, whereas in the presence of CCCP (unlimited H^+ conductance), the rate of fluorescence quenching (ΔQ/min) measured the maximal intrinsic K^+ conductance of the membrane. In the presence of both ionophores, the total quenching amplitude (% of the starting fluorescence) indicated the amount of sealed vesicles [16,6].

In our previous study, we did all the necessary control experiments and demonstrated that the ΔpH, and the respective quenching of AO fluorescence, develops only in sealed vesicles, and that the quenching amplitude is proportional to the amount of vesiculated membranes in the assay [6].

2.6. Presentation of data and statistical analysis

The data are shown by the representative original recordings and/or by means ± SD (EPR data) or means ± SEM (ion conductances) from measurements in 4 (EPR data) to 13 (ion conductances) independent preparations of membrane organelles. Discriminant function analysis (Statistica 6.0, StatSoft. Inc., DFA module) was applied in order to choose the EPR fitting parameters that contribute most to the discrimination between three types of organelle membranes and to check the discriminatory power by post hoc classification of cases. Wilk's lambda for the overall discrimination denotes statistical significance of the discriminatory power of the model; it is computed as the ratio of the determinant of the within groups variance over the determinant of the total variance matrix. The model can be tested through the post hoc classification of the cases into discriminated groups. The distribution of spectral parameter values was described by means ± SD and the comparisons performed by one-way or factorial analysis of variance (Statistica 6.0, StatSoft.Inc., ANOVA module), depending on the number of parameters analyzed. The data for ion conductances were statistically evaluated using the Student t test. In all statistical tests the significancy was determined at the 0.05 level.

3. Results

3.1. Comparison of dynamics and ordering in the membrane organelles from rat kidney cortex

The BBM, BLM, and endosomes are associated with different well-defined roles in kidney function [30]. They contain different protein and lipid composition as well as protein/lipid ratio [17,18] and therefore are expected to be discriminated in the dynamics and ordering of the lipid domains.

The lipophilic spin probe MeFASL(10,3), incorporated into the membranes isolated from the kidney cortex of the intact, adult rats exhibited well-defined stable EPR spectra. Since the spectra did not show spin-exchange broadening, we assumed that the recorded signals represented evenly labeled lipid bilayer (laterally and transversally). The spectra were analyzed by a simulation method developed for lipid bilayers. The spectral line shapes reflect structure and dynamics of micro-environment of the probe in a membrane; the parameters used in the simulation analysis estimate the fluidity of the probed membrane. In the present study, all the spectra were complex and could not be fitted in a satisfactory manner with a single calculated line shape. Our best attempt to fit a representative spectrum with a single line is presented in Fig. 1A.

A reasonably good fitting of the spectra was achieved assuming three spectral components, selected in the following way. First, the parameters for the most ordered component (I) were obtained by adjusting the outer hyperfine splitting. Then the parameters for the most fluid component (III) were taken from the simulation of the inner hyperfine splitting. Finally, the fitting parameters for intermediate component (II) were deduced from the minimization of the χ^2 value. Once the components are defined, the recorded spectra for the three membrane organelles are reproduced just by adjusting the weighting factors to reach minimal χ^2 value. Fig. 1B shows the fit of the experimental spectrum from Fig. 1A with the use of the above procedure. There is an obvious difference in the goodness of the fit, as indicated by the plot of χ^2, shown under the respective spectra.

The comparison of the recorded spectra with the spectra reconstructed by appropriate summation of the constituents I, II, and III, for the three organelle membranes are shown in Fig. 2.

Most of the fitting parameters showed slight temperature dependence, except the order parameters for component III. Marked temperature-dependent decrease was observed for parameters S_3 and τ_{20}, as shown in Table 1. This table also shows the data related to Cd-treated rats (discussed later). The weights of components exhibited even stronger temperature

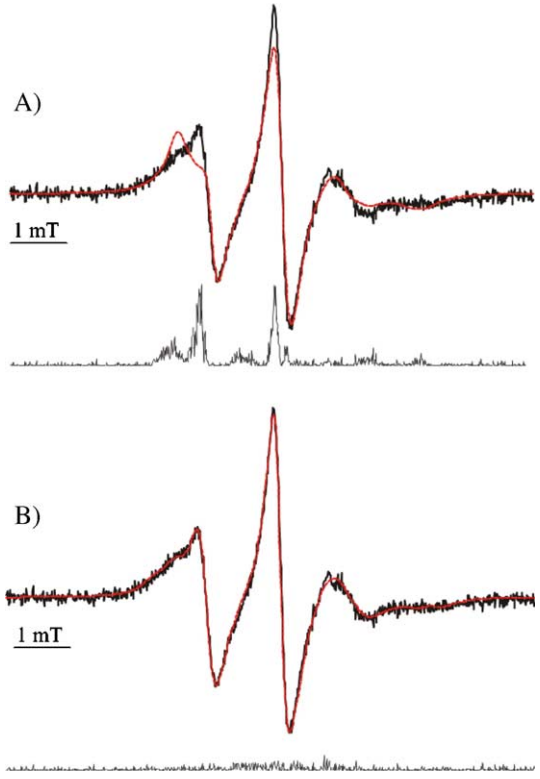

Fig. 1. The best theoretical fit (red lines) of the EPR spectrum of brush-border membrane, recorded at 32 °C (black lines), with single component (A) and with three components (B). Below the spectra the χ^2 value (as a measure of the goodness of the respective fit) is plotted.

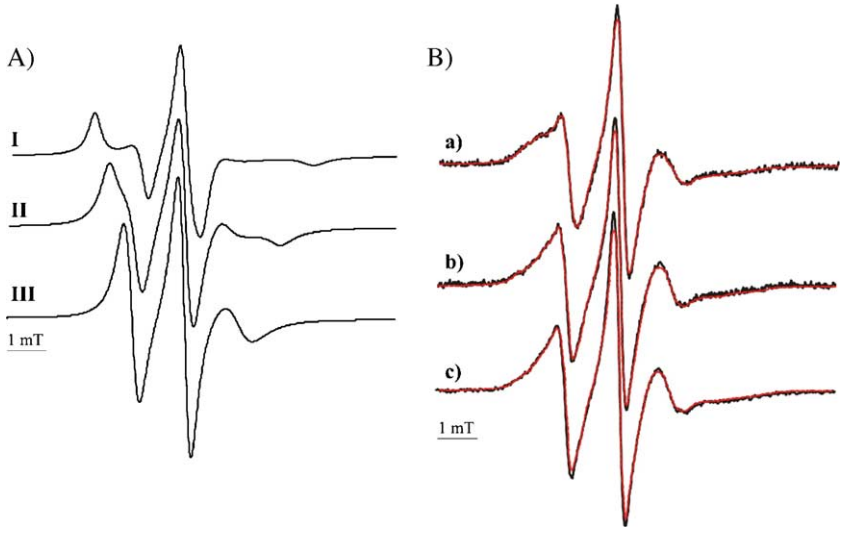

Fig. 2. (A) Spectral components I, II, and III calculated to fit experimental ESR spectra of spin probe MeFASL (10,3) incorporated into three different organelle membranes, at 32 °C. (B) Calculated complex spectra (red lines) superimposed to experimental spectra (black lines) of three membrane types; (a) brush-border membrane, calculated spectrum consists of 66%I+ 23%II+ 11%III; (b) basolateral membrane, calculated spectrum consists of 54%I+ 29%II+ 17%III; (c) endocytotic vesicles, calculated spectrum consists of 42%I+ 32%II+ 26%III.

dependence and better distinction between different membrane types, as shown in Fig. 3.

In order to quantitatively precise the model for differentiation of the organelles according to their spectral parameters, a discriminant function analysis was applied. Every spectrum was described using S_3, S_1, τ_{20}, τ_{22}, and w for all three spectral components. For spectral component I parameters, a good discriminative power was shown for ordering S_3 (Wilk's $\lambda=0.299$, $P=0.031$) and weight parameter w (Wilk's $\lambda=0.336$, $P=0.019$). Correct classification of cases into membrane types according to the observed parameters was highest at 27 and 32 °C (Table 2). Discrimination for spectral component II parameters was best achieved through S_3 (Wilk's $\lambda=0.367$, $P=0.013$), rotational correlation times τ_{20} (Wilk's $\lambda=0.204$, $P=0.016$), τ_{22} (Wilk's $\lambda=0.328$, $P=0.022$) and weight w parameter (Wilk's $\lambda=0.324$, $P=0.023$), with 100% correct classification at 27 and 42 °C (Table 2). The best discriminative power of spectral component III were again rotational correlation times τ_{20} (Wilk's $\lambda=0.256$, $P=0.050$), τ_{22} (Wilk's $\lambda=0.575$, $P=0.001$) and weight w parameter (Wilk's $\lambda=0.324$, $P=0.023$), with the highest percentage of correctly classified cases at 32 and 37 °C.

It is seen that the overall discrimination for the different membrane types based on the three spectral component's parameters is, at most temperatures, very good.

3.2. EPR comparison of BBM from untreated and Cd-treated rats

BBM, isolated from the control and Cd-treated animals, were spin labeled and the respective EPR spectra were recorded and analyzed. The specimens of the Cd-treated and the control animals differed, as illustrated in Fig. 4. The results of the fitting procedure for the membranes of the Cd-treated

Table 1
Order parameters and rotational correlation times of calculated spectral components (I, II and III) at various temperatures for three types of organelle membranes, and for Cd-treated membranes[a]

Sp.comp.	BLM			EV			BBM			Cd-treated BBM		
	I	II	III	I	II	III	I	II	III	I	II	III
t (°C)	Order parameter S_3											
22	0.66±0.04	0.40±0.03	0.12±0.01	0.68±0.01	0.40±0.01	0.12±0.01	0.68±0.01	0.40±0.02	0.11±0.01	0.62±0.01	0.46±0.01	0.12±0.01
27	0.66±0.02	0.37±0.01	0.12±0.01	0.67±0.01	0.39±0.01	0.11±0.01	0.65±0.02	0.38±0.03	0.12±0.01	0.60±0.01	0.45±0.03	0.10±0.0
32	0.65±0.01	0.37±0.01	0.12±0.0	0.65±0.01	0.35±0.01	0.12±0.01	0.65±0.01	0.36±0.03	0.12±0.01	0.61±0.01	0.42±0.03	0.10±0.0
37	0.61±0.02	0.33±0.02	0.12±0.01	0.62±0.0	0.33±0.02	0.12±0.0	0.61±0.01	0.33±0.01	0.12±0.01	0.59±0.01	0.39±0.01	0.10±0.0
42	0.59±0.01	0.30±0.05	0.11±0.01	0.61±0.01	0.31±0.01	0.12±0.01	0.59±0.0	0.32±0.01	0.12±0.0	0.59±0.0	0.37±0.01	0.10±0.0
Rotational correlation time τ_{20}/ns												
22	2.88±0.05	1.80±0.08	1.80±0.18	2.86±0.05	2.13±0.25	1.89±0.07	2.81±0.08	2.22±0.45	1.75±0.17	2.30±0.18	1.75±0.17	1.75±0.17
27	2.68±0.15	1.83±0.09	1.75±0.06	2.84±0.06	1.89±0.07	1.87±0.05	2.75±0.13	1.92±0.05	1.68±0.09	2.15±0.15	1.68±0.15	1.65±0.12
32	2.48±0.09	1.68±0.09	1.63±0.05	2.58±0.06	1.81±0.08	1.85±0.06	2.48±0.27	1.97±0.05	1.77±0.05	2.0±0.17	1.52±0.12	1.52±0.12
37	2.25±0.13	1.63±0.12	1.63±0.05	2.18±0.06	1.79±0.11	1.75±0.11	2.37±0.12	1.80±0.11	1.77±0,05	2.0±0.17	1.45±0.17	1.43±0.15
42	1.90±0.10	1.30±0.10	1.20±0.0	1.88±0.06	1.42±0.09	1.37±0.09	2.27±0.25	1.60±0.10	1.46±0.21	1.95±0.18	1.45±0.17	1.35±0.19

[a] Presented are means±SD from four samples of each membrane type.

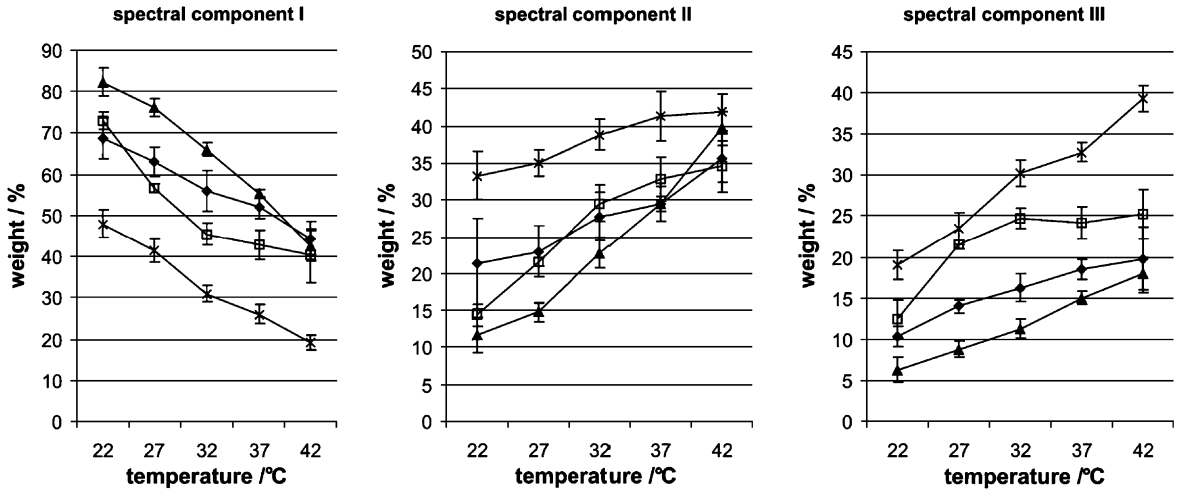

Fig. 3. Temperature dependence of weights of spectral components for three types of organelle membranes—basolateral (BLM—♦), brush border (BBM—▲) and endocytotic vesicles (EV—□), as well as of cadmium treated brush border membranes (Cd-BBM–X) for comparison with BBM (▲) as a control. The data collected from four samples of each type of membrane are presented as mean values with SD.

animals are summarized in Table 1, together with the data for all kidney membrane types of untreated rats. The BBM vesicles isolated from Cd-intoxicated animals revealed a few differences from the respective membranes of untreated animals (control). BBM vesicles from Cd-treated rats showed lower order (smaller S_3) of component I and higher order of component II than the vesicles of untreated rats. As judged from the values of correlation time $\tau_{20,}$ the former vesicles are characterized by faster rotation around the long molecular axis, indicating less restriction in the rotational motion. The overall change in spectral parameters indicates that the spectral component II in BBM from Cd-treated rats is characterized with better ordering (an average increase of S_3 for about 15%, differences being statistically significant in the whole temperature range) indicating smaller average amplitudes of motion and faster mobility (decrease of rotational correlation time τ_{20} for 10–20%, differences being statistically significant in the 27–37 °C temperature range). Even more noted difference is in the proportion of the domains in the two systems. Spectral component I of the BBM vesicles of the Cd-treated animals was present at significantly lower proportion, while components II and III were present with higher proportion at all temperatures (Fig. 3). Generally, it seems that the Cd treatment introduced slight disordering and more freedom in the rotational motion into BBM and a partial transformation of component I into components II and III.

Table 2
Results of discriminant analysis—percentage of correct post hoc classification into membrane types based on spectral parameters deduced from fitting procedure

Spectral component	Membrane type	Temperature/°C					Average
		22	27	32	37	42	
I	BLM	75	75	100	75	67	78
	EV	75	100	100	100	75	90
	BBM	88	100	88	75	88	88
	average	80	92	96	83	77	86
II	BLM	100	100	100	75	100	95
	EV	100	100	63	50	100	83
	BBM	75	100	100	88	100	93
	average	92	100	88	71	100	90
III	BLM	0	75	75	75	100	65
	EV	75	50	75	100	50	70
	BBM	88	88	100	100	88	93
	average	54	71	83	92	79	76

3.3. Ion conductance in isolated BBM from control and Cd-treated rats

The renal cortical BBM vesicles from control or Cd-treated rats, preloaded with KCl-buffer and diluted in the same, AO-containing buffer (with both ionophores present), showed only a limited and similar time-dependent drift of the fluorescence (Fig. 5, $K^+_{in=out}$). However, the vesicles diluted in TMACl-buffer that contained a K^+ ionophore valinomycin (VAL), exhibited a transient, time-dependent quenching of AO fluorescence due to K^+ diffusion potential-driven intravesicular uptake of protons via intrinsic conductive pathways in the membrane, and

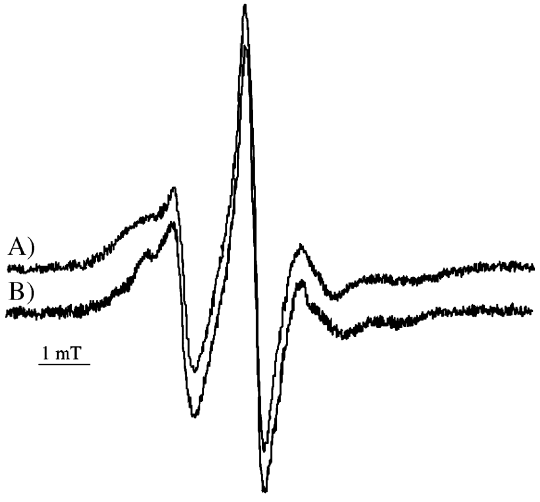

Fig. 4. Experimental spectra of control and cadmium-treated brush border membrane at 32 °C.

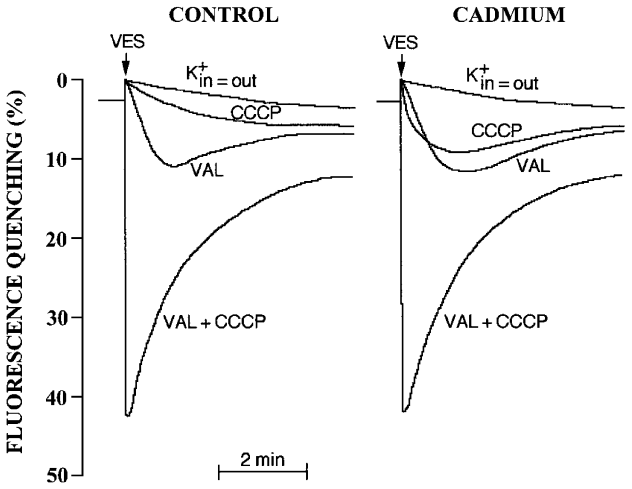

Fig. 5. Measured H^+ and K^+ conductances in renal cortical BBM vesicles isolated from the control and Cd-treated rats. Vesicles preloaded with KCl-buffer were diluted in the same ($K^+_{in=out}$) or TMACl-buffer (all other recordings) that contained acridine orange and either K+ ionophore valinomycin (VAL) or protonophore CCCP, or both ionophores (VAL+CCCP). Shown are the redrawn original recordings.

generation of the transmembrane ΔpH. As shown in Fig. 5 and Table 3, the initial rates of fluorescence quenching in the presence of valinomycin in BBM vesicles from both animal groups were similar, indicating similar maximal intrinsic conductances for H^+ in both membrane preparations. On the contrary, in the presence of protonophore CCCP, the development of transmembrane ΔpH (fluorescence quenching) was limited by maximal intrinsic conductance of the membrane for K^+; as shown in Fig. 5 and Table 3, the initial rates of fluorescence quenching in the presence of CCCP were 4- to 5-fold higher in the BBM vesicles from Cd-treated animals. A deep but similar quenching amplitude in the presence of both ionophores (VAL+CCCP), when unlimited conductances for both ions generated a fast and strong fluorescence quenching (maximal transmembrane ΔpH), indicated that the proportion of vesicles in both membrane preparations was similar, thus excluding the possibility that the observed difference in K^+ conductances was caused by different vesiculation states.

4. Discussion

Whereas various aspects of protein-related transports and their regulations in cell membranes and intracellular organelles in the mammalian kidney and other organs have been extensively studied, the roles and characteristics of the lipid phase in these membrane organelles in various (patho)physiological and toxicological states have attracted much less attention. In this work, we have shown that the EPR spectroscopy with appropriate spin-labeled membrane lipids can be used for discriminatory characterization of the three defined membrane organelles from the renal cortex, e.g., BBM, BLM, and endocytic vesicles, which could be isolated to the reasonable purity using the well established and widely used methods. Previous biochemical studies indicated characteristic patterns and clear distinction in the relative content of various (phospho)lipids and protein/lipid ratios in the limiting membranes of these organelles [17,18]. The optimal parameters were then used to test if Cd-treatment in rats affects the characteristics of the lipid phase in the renal cortical BBM.

The results of simulation of the experimental EPR spectra from the spin labeled lipid phase of BBM, endocytic vesicles, and BLM showed that in all cases a minimum of three spectral components (I, II, and III, respectively) was required to obtain a reasonable calculated fit. That suggests that in the lipid phase of these membrane types there are at least three different types of domains, sensed by different motional restrictions of the applied lipophylic spin probe.

In the early EPR spin labeling study of BBM and BLM vesicles Hise and coworkers [17] assumed and analyzed just one type of lipid domains, probably identical to our domain I. On the other hand, there are methods that allow for any degree of heterogeneity of the membranes and related EPR spectra [31–33]. In practical application, these methods reduce to grouping of contributions to only few relevant groups [33], something similar to our initial standpoint.

The lipid domains, detected and interpreted in the EPR spectra, should be considered as parts of a membrane having different structural and dynamical properties. Their dynamic properties and their stability are mainly determined by the lipid–lipid or lipid–protein interactions [34]. The domains are distinguished mainly by order parameter S_3. In the entire temperature range applied the three types of membrane vesicles differed in their S_3 values (see Table 1), suggesting the domains to remain structurally consistent. Based on the obvious difference in ordering, we call them most ordered and least fluid (I), intermediate (II) and least ordered and most fluid (III) domains.

The three types of membranes essentially do not differ with respect to the spectral parameters, but they do in their weights or proportions, in which they contribute to the whole spectrum. The weight of a spectral component indicates the proportion to which the domain occupies the membrane surface area. The BBM are distinguished from the BLM [17,18] and endocytotic vesicles [18] mostly by having the highest proportion of most ordered domain and lowest proportion of most fluid domain, indicating lowest overall lipid phase fluidity among the investigated membranes. This is in accordance with the known protein/lipid ratio in BBM, which is larger than in BLM [17,18] or EV [18]. Also, the largest proportion of the most fluid domain in endocytic vesicles demonstrates the highest overall fluidity among the investigated membranes, the conclusion also previously reached on the basis of comparatively higher

Table 3
H^+ and K^+ conductances in renal cortical brush-border membrane vesicles isolated from control and Cd-treated rats[a]

Parameter	Control	Cd-treated	P
H^+ conductance (ΔQ/min)	174±9.8	170±13.1	N.S.
K^+ conductance (ΔQ/min)	14±1.8	62.3±7.8	<0.001
Quenching amplitude (%)	48±1.3	45±1.2	N.S.

[a] The results are expressed as mean±SEM for 12 control and 13 Cd-treated rats.

presence of phospholipids in their membrane [18]. The EPR data (this report) and biochemical data for BLM [18] are in between the BBM and endosomal data. Thus, the EPR spectroscopy not only closely correlated with the previously reported biochemical data on lipid profiles in membrane organelles isolated from the same tissue, but also suggests that the EPR spectroscopy could be used as a tool for distinction and/or specification of various types of plasma membranes and intracellular organelles from the mammalian kidney and, possibly, other organs. The discriminant analysis of spectroscopic parameters revealed conditions under which almost 100% correct classification of the membrane (organelle) type is achievable.

It is now quite clear that the overall membrane lipid dynamics and ordering largely depend on the lipid/protein ratio, defining the strength of the lipid–protein interactions. In that respect the membrane lipids could be classified into three groups: annular, non-annular and bulk lipids. Most aspects of the lipid interactions and ordering in biological membranes have recently been reviewed [35–39]. The former two groups of lipids participate in a direct, non-covalent interaction with membrane proteins and are considered to form a first shell, surrounding the protein. An individual lipid molecule remains in the annular shell or in the non-annular binding for only a short period of time. The lipids of the third group represent a solvent and are even freer in their dynamics. Thus, it is quite probable that the above three groups of membrane lipids correspond to the three EPR spectral components presented in this work.

Cadmium treatment of rats induced changes in structural and dynamical properties of the lipid bilayers of isolated BBM vesicles. The EPR data demonstrated increased molecular mobility, resulting in the membrane fluidizing effect. From our largely phenomenological data it is not possible to explain the molecular base for the observed fluidity differences between BBM from control and Cd-treated animals. Although it is generally accepted that due to its high affinity for SH groups [40] Cd binds avidly to various proteins and thus interferes with their structure and function, as illustrated by numerous examples [2–5,8–10,14,41]. An old literature demonstrated that Cd could also bind to various (phospho)lipids, such as lecithin, phosphatidylserine and phosphatidyletanolamine, that are usual constituents in the cell membranes, with an affinity which is about 100-fold higher than that of calcium [40,42]. Such a direct interaction of Cd with phospholipids may affect the mobility of lipids and proteins, and consequently, the state of membrane fluidity and its function. A support for such a direct interaction of Cd with the cell membrane phospholipids in vivo comes from the research on streptozotocin-induced- or spontaneously-diabetic rats. These rats are more sensitive to Cd-induced nephrotoxicity than the healthy animals [43], most probably due to interaction of Cd with the more abundant myelin lipid phase that increases fluidity of the cell membrane in peripheral neurons [44]. Regardless of the cause and consequence, the change of either protein or lipid domains in the membranes may be via the lipid–protein interactions manifested in alterations of both domains [36–39,45].

Alternatively, following in vivo treatment, Cd may change the lipid profile in the membranes by chemical changes. Numerous recent publications have indicated that Cd (and some other toxic metals) can induce oxidative stress and enhance production of ROS that cause peroxidation of lipids in kidney and other organs [11,19–22,46,47]. Oxidation of lipids could change biophysical properties of the lipid phase, such as the observed increased fluidity of the renal cortical BBM isolated from the Cd-treated rats. Yet another (or complementary) mechanisms of Cd action upon the lipid phase in renal BBM could be suggested. Cadmium was found to induce phosphatidylinositol (PI) hydrolysis [48]. Since PI is known to serve as lipid anchor by covalent binding to some outer surface membrane proteins [49], the PI hydrolysis could provoke a release of those proteins from the membrane. Finally, our recent studies showed that the treatment of rats with Cd or Cd-metallothionein causes in the renal cortical BBM a dramatic, time-dependent decrease in the abundance of some transport proteins due to diminished recycling of intracellular vesicles [5,6,13,14]; the loss of specific proteins might affect the protein/lipid ratio and lipid–protein interactions, leading to change of lipid order and mobility.

We have assumed that the observed Cd-induced changes in the BBM lipid domain, revealed by EPR could be reflected in the permeability of the membrane to ions. Indeed, as demonstrated in our fluorescence studies, the BBM from Cd-treated animals exhibited 4- to 5-fold higher conductance for K^+, whereas the conductance for H^+ remained unchanged. This indicates that in Cd-treated rats the ion permeabilities of the BBM were selectively affected, and did not result from a general loss of membrane integrity, as observed in in vitro treated isolated rat renal cortical BBM and BLM by Cd and various other nephrotoxic metals [16]. A high K^+ conductance may reflect the Cd-induced changes in the lipid phase (higher fluidity) of BBM, observed with the EPR spectroscopy. A change in the lipid phase might differently affect different proteins, namely their biological functions. Thus, in the in vitro studies of isolated rabbit proximal tubule fragments, the silver ion strongly increased the permeability of the cell membrane for K^+ [50], whereas in cultured renal epithelial cells, Cd caused an increased permeability of the cell membrane for Cl^- [51]. An increased permeability of BBM for K^+, as found in our Cd-treated rats, may in proximal tubule cells dissipate transmembrane K^+ gradients and interfere with generation and maintenance of the cell membrane potential and may thus contribute to the initial nephrotoxic actions of Cd in these cells.

Acknowledgements

The authors thank Mrs. Eva Heršak for the help in treating animals with cadmium and in isolation of membrane organelles. This work was supported by grants No. 0022011 (I.S.) and No. 006421 (J.N.H.) from the Ministry of Science, Education and Sports, Republic of Croatia.

References

[1] Y.K. Kim, J.K. Choi, J.S. Kim, Y.S. Park, Changes in renal function in cadmium-intoxicated rats, Pharmacol. Toxicol. 63 (1988) 342–350.

[2] K.R. Kim, H.Y. Lee, C.K. Kim, Y.S. Park, Alteration of renal amino acid transport system in cadmium-intoxicated rats, Toxicol. Appl. Pharmacol. 106 (1990) 102–111.
[3] H.Y. Lee, K.R. Kim, Y.S. Park, Transport kinetics of glucose and alanine in renal brush-border membrane vesicles of cadmium-intoxicated rabbits, Pharmacol. Toxicol. 69 (1991) 390–395.
[4] D.W. Ahn, Y.S. Park, Transport of inorganic phosphate in renal cortical brush-border membrane vesicles of cadmium-intoxicated rats, Toxicol. Appl. Pharmacol. 133 (1995) 239–243.
[5] C.M. Herak-Kramberger, B. Spindler, J. Biber, H. Murer, I. Sabolic, Renal type II Na/Pi-cotransporter is strongly impaired whereas the Na/sulphate-cotransporter and aquaporin 1 are unchanged in cadmium-treated rats, Pfluegers Arch. Eur. J. Physiol. 432 (1996) 336–344.
[6] C.M. Herak-Kramberger, D. Brown, I. Sabolic, Cadmium inhibits vacuolar H+-ATPase and endocytosis in rat kidney cortex, Kidney Int. 53 (1998) 1713–1726.
[7] R.J. Condron, C.J. Schroen, A.T. Marshall, Morphometric analysis of renal proximal tubules in cadmium-treated rats, J. Submicrosc. Cytol. Pathol. 26 (1994) 51–58.
[8] R.K.H. Kinne, H. Schutz, E. Kinne-Saffran, The effect of cadmium chloride in vitro on sodium-glutamate cotransport in brush border membrane vesicles isolated from rabbit kidney, Toxicol. Appl. Pharmacol. 135 (1995) 216–221.
[9] K. Sato, Y. Kusaka, K. Okada, Direct effect of cadmium on citrate uptake by isolated rat renal brush border membrane vesicles, Toxicol. Lett. 80 (1995) 161–165.
[10] W. Ahn, Y.K. Kim, K.R. Kim, Y.S. Park, Cadmium binding and sodium-dependent solute transport in renal brush-border membrane vesicles, Toxicol. Appl. Pharmacol. 154 (1999) 212–218.
[11] Z.A. Shaikh, T.T. Vu, K. Zaman, Oxidative stress as a mechanism of chronic cadmium-induced hepatotoxicity and renal toxicity and protection by antioxidants, Toxicol. Appl. Pharmacol. 154 (1999) 256–263.
[12] F. Thevenod, J.M. Friedmann, Cadmium-mediated oxidative stress in kidney proximal tubule cells induces degradation of Na+/K+-ATPase through proteasomal and endo-/lysosomal proteolytic pathways, FASEB J. 13 (1999) 1751–1761.
[13] I. Sabolic, C.M. Herak-Kramberger, M. Blanusa, D. Brown, Loss of brush-border proteins in cadmium-induced nephrotoxicity in rat, Period. Biol. 102 (2000) 33–41.
[14] I. Sabolic, M. Ljubojevic, C.M. Herak-Kramberger, D. Brown, Cd-MT causes endocytosis of brush-border transporters in rat renal proximal tubules, Am. J. Physiol.: Renal Physiol. 283 (2002) F1389–F1402.
[15] I. Sabolic, C.M. Herak-Kramberger, D. Brown, Subchronic cadmium treatment affects the abundance and arrangement of cytoskeletal proteins in rat renal proximal tubule cells, Toxicology 165 (2001) 205–216.
[16] C.M. Herak-Kramberger, I. Sabolic, The integrity of renal cortical brush-border and basolateral membrane vesicles is damaged in vitro by nephrotoxic heavy metals, Toxicology 156 (2001) 139–147.
[17] M.K. Hise, W.W. Mantulin, E.J. Weinman, Fluidity and composition of brush border and basolateral membranes from rat kidney, Am. J. Physiol. 247 (1984) F434–F439.
[18] F. Bode, K. Baumann, R. Kinne, Analysis of the pinocytic process in rat kidney: II. Biochemical composition of pinocytic vesicles compared to brush border microvilli, lysosomes and basolateral plasma membranes, Biochim. Biophys. Acta 433 (1976) 294–310.
[19] S. Sakar, P. Yadav, R. Trivedi, A.K. Bansal, D. Bhatnagar, Cadmium-induced lipid peroxidation and the status of the antioxidant system in rat tissues, J. Trace Elem. Med. Biol. 9 (1995) 144–149.
[20] S.J. Yiin, C.L. Chern, J.Y. Sheu, W.C. Tseng, T.H. Lin, Cadmium-induced renal lipid peroxidation in rats and protection by selenium, J. Toxicol. Environ. Health 57 (1999) 403–413.
[21] R. Karmakar, M. Chatterjee, Cadmium-induced time-dependent oxidative stress in liver of mice: a correlation with kidney, Environ. Toxicol. Pharmacol. 6 (1998) 201–207.
[22] E. Casalino, G. Calzaretti, C. Salano, C. Landriscina, Molecular inhibitory mechanisms of antioxidant enzymes in rat liver and kidney by cadmium, Toxicology 179 (2002) 37–50.
[23] J. Biber, B. Stieger, W. Haase, H. Murer, A high yield preparation for rat kidney brush border membranes; different behaviour of lysosomal markers, Biochim. Biophys. Acta 647 (1981) 169–176.
[24] V. Scalera, Y.K. Huang, B. Hildmann, H. Murer, A simple isolation method for basal-lateral plasma membranes from rat kidney cortex, Membr. Biochem. 4 (1981) 49–64.
[25] I. Sabolic, G. Burckhardt, ATP-driven proton transport in vesicles from rat kidney cortex, Methods Enzymol. 191 (1990) 505–520.
[26] I. Sabolic, G. Burckhardt, Proton pathways in rat renal brush-border and basolateral membranes, Biochim. Biophys. Acta 734 (1983) 210–220.
[27] M.M. Bradford, A rapid and sensitive method for the quantization of microgram quantities of protein utilizing the principle of protein-dye binding, Anal. Biochem. 72 (1976) 248–254.
[28] H. Schindler, J. Seelig, EPR spectra of spin labels in lipid bilayers, J. Chem. Phys. 59 (1973) 1841–1850.
[29] M. Zuvic-Butorac, U. Batista, M. Schara, ESR spectra of cell membranes, Period. Biol. 103 (2001) 235–240.
[30] D. Brown, I. Sabolic, S. Breton, Membrane macro- and microdomains in electrolyte transporting epithelia: structure–function correlations, in: D.W. Seldin, G. Giebisch (Eds.), The Kidney, Lippincott Williams and Wilkins, Philadelphia, 2000, pp. 655–684.
[31] J. Štrancar, M. Šentjurc, M. Schara, Fast and accurate characterization of biological membranes by EPR spectra simulation of nitroxides, J. Magn. Reson. 142 (2000) 253–265.
[32] J. Štrancar, T. Koklič, Z. Arsov, Soft picture of lateral homogeneity in biomembranes, J. Membr. Biol. 196 (2003) 135–146.
[33] J. Štrancar, Spin label EPR-based characterization of biosystem complexity, J. Chem. Inf. Model. 45 (2005) 394–406.
[34] M. Zuvic-Butorac, P. Muller, T. Pomorski, J. Libera, A. Herrmann, M. Schara, Lipid domains in the exoplasmic and cytoplasmic leaflet of the human erythrocyte membrane: a spin label approach, Eur. Biophys. J. 28 (1999) 302–311.
[35] A.G. Lee, Lipid–protein interactions in biological membranes: a structure perspective, Biochim. Biophys. Acta 1612 (2003) 1–40.
[36] H. Palsdottir, C. Hunte, Lipids in membrane protein structure, Biochim. Biophys. Acta 1666 (2004) 2–18.
[37] P.H.M. Lommerse, H.-P. Spaink, T. Schmidt, In vivo plasma membrane organization: results of biophysical approaches, Biochim. Biophys. Acta 1664 (2004) 119–131.
[38] M.Ø. Jensen, O.G. Mouritsen, Lipids influence protein function—The hydrophobic matching hypothesis revisited, Biochim. Biophys. Acta 1666 (2004) 118–141.
[39] D. Marsh, T. Páli, The protein–lipid interface: perspectives from magnetic resonance and crystal structures, Biochim. Biophys. Acta 1666 (2004) 118–141.
[40] B.L. Vallee, D.D. Ulmer, Biochemical effects of mercury, cadmium, and lead, Ann. Rev. Biochem. 41 (1972) 91–128.
[41] K. Park, K.R. Kim, J.Y. Kim, Y.S. Park, Effect of cadmium on Na–Pi cotransport kinetics in rabbit renal brush-border membrane vesicles, Toxicol. Appl. Pharmacol. 145 (1997) 255–259.
[42] M. Webb, Interactions of cadmium with cellular components, in: M. Webb (Ed.), The Chemistry, Biochemistry and Biology of Cadmium, Elsevier, Amsterdam, 1979, pp. 285–340.
[43] T.Y. Jin, G. Nordberg, J. Sehlin, H. Wallin, S. Sandberg, The susceptibility to nephrotoxicity of streptozotocin-induced diabetic rats subchronically exposed to cadmium chloride in drinking water, Toxicology 142 (1999) 69–75.
[44] M. Zuvic-Butorac, J. Križ, A. Simonić, M. Schara, Fluidity of the myelin sheath in the peripheral nerves of diabetic rats, Biochim. Biophys. Acta Mol. Basis Dis. 1537 (2001) 110–116.
[45] A.G. Lee, How lipids affect the activity of integral membrane proteins, Biochim. Biophys. Acta 1666 (2004) 62–87.
[46] E.L.B. Novelli, A.M. Lopes, A.S. Rodrigues, J.L.V. Novelli, B.O. Ribas, Superoxide radical and nephrotoxic effect of cadmium exposure, Int. J. Environ. Health Res. 9 (1999) 109–116.
[47] M. Karbownik, E. Gitto, A. Lewinski, R.J. Reiter, Induction of lipid peroxidation in hamster organs by the carcinogen cadmium: amelioration by melatonin, Cell Biol. Toxicol. 17 (2001) 33–40.

[48] J. Bingham-Smith, S.D. Dwyer, L. Smith, Cadmium evokes inositol phosphate formation and calcium mobilization, J. Biol. Chem. 264 (1989) 7115–7118.
[49] I.W. Caras, G.N. Weddell, M.A. Davitz, V. Nussenzweig, D.W. Martin, Signal for attachment of a phospholipid membrane anchor in decay accelerating factor, Science 238 (1987) 1280–1283.
[50] B.C. Kone, M. Kaleta, S.R. Gullans, Silver ion (Ag^+)-induced increases in cell membrane K+ and Na+ permeability in the renal proximal tubule: reversal by thiol reagents, J. Membr. Biol. 102 (1988) 11–19.
[51] B. Faurskov, H.F. Bjerregaard, Effect of cadmium on active ion transport and cytotoxicity in cultured renal epithelial cells (A6), Toxicol. In Vitro 11 (1997) 717–722.